



**HAL**  
open science

# Investigation of induction times, activity, selectivity, interface and mass transport in solvent-free epoxidation by H<sub>2</sub>O<sub>2</sub> and TBHP: a study with organic salts of the [PMo<sub>12</sub>O<sub>40</sub>]<sup>3-</sup> anion

Béatrice Guérin, Daniel Mesquita Fernandes, Jean-Claude Daran, Dominique Agustin, Rinaldo Poli

## ► To cite this version:

Béatrice Guérin, Daniel Mesquita Fernandes, Jean-Claude Daran, Dominique Agustin, Rinaldo Poli. Investigation of induction times, activity, selectivity, interface and mass transport in solvent-free epoxidation by H<sub>2</sub>O<sub>2</sub> and TBHP: a study with organic salts of the [PMo<sub>12</sub>O<sub>40</sub>]<sup>3-</sup> anion. *New Journal of Chemistry*, 2013, 37 (11), pp.3466. <10.1039/C3NJ00523B>. <hal-02907980>

**HAL Id: hal-02907980**

**<https://hal.science/hal-02907980v1>**

Submitted on 2 Mar 2021

HAL is a multi-disciplinary open access archive for the deposit and dissemination of scientific research documents, whether they are published or not. The documents may come from teaching and research institutions in France or abroad, or from public or private research centers.

L'archive ouverte pluridisciplinaire HAL, est destinée au dépôt et à la diffusion de documents scientifiques de niveau recherche, publiés ou non, émanant des établissements d'enseignement et de recherche français ou étrangers, des laboratoires publics ou privés.



HAL Authorization

Cite this: DOI: 10.1039/c0xx00000x

www.rsc.org/xxxxxx

ARTICLE TYPE

## Investigation of induction times, activity, selectivity, interface and mass transport in solvent-free epoxidation by H<sub>2</sub>O<sub>2</sub> and TBHP: a study with organic salts of the [PMo<sub>12</sub>O<sub>40</sub>]<sup>3-</sup> anion

Béatrice Guérin<sup>a,b</sup>, Daniel Mesquita Fernandes<sup>a,b</sup>, Jean-Claude Daran<sup>a,b</sup>, Dominique Agustin<sup>\*a,b</sup> and Rinaldo Poli<sup>\*a,c</sup>

Received (in XXX, XXX) Xth XXXXXXXXXX 20XX, Accepted Xth XXXXXXXXXX 20XX DOI: 10.1039/b000000x

The phosphomolybdate salts Q<sub>3</sub>[PMo<sub>12</sub>O<sub>40</sub>] [Q = tetra-*n*-butylammonium (TBA), *n*-butylpyridinium (BP), cetylpyridinium (CP)] have been used as catalysts for the epoxidation of cyclooctene under organic solvent-free conditions, using H<sub>2</sub>O<sub>2</sub> or *t*-BuOOH (TBHP) in water as oxidants, and compared with the BP salt of the analogous tungsten derivative, (BP)<sub>3</sub>[PW<sub>12</sub>O<sub>40</sub>]. High catalytic activities have been recorded down to very low catalyst loadings (2 ppm). The activity and selectivity depend on the oxidant and cation nature. The dominant process appears to be homogeneous and this rationalizes, together with the evolution of the phase equilibria, the presence of an induction period for the epoxidation by H<sub>2</sub>O<sub>2</sub> and the evolution of the epoxide selectivity. The recovered catalysts are reusable and exhibit equivalent reactivity.

### Introduction

Among the Green chemistry principles, catalysis plays a key role.<sup>1-3</sup> In addition to obvious economical reasons related to catalyst loss and to separation and/or regeneration costs, efficient catalyst recovery and recycling also has a positive impact on the environment. The catalyst must be active and stable under catalytic conditions, its leaching should be minimal and its recovery must be facile. Both economical and environmental concerns are also leading industry to consider the implementation of solvent-free operating conditions.<sup>4</sup>

Oxidation reactions carried out in the absence of organic solvents have received so far little attention.<sup>5-12</sup> We are currently investigating solvent-free epoxidation. Our investigations have so far addressed catalysts based on molybdenum(VI) and vanadium(V) oxo-complexes surrounded by tridentate ligands.<sup>13-15</sup> One particular molybdenum complex, [MoO<sub>2</sub>L<sup>1</sup>(MeOH)], where L<sup>1</sup> is a Schiff base ONS-type tridentate ligand derived from pyridoxal thiosemicarbazone, was found to be very active thus leading to satisfactory conversions at very low metal content (0.05 mol% [Mo] vs. substrate). Other molybdenum and vanadium complexes, [MoO<sub>2</sub>L<sup>2</sup>]<sub>2</sub> and [VOL<sup>2</sup>]<sub>2</sub>O (L<sup>2</sup> = Schiff base ONO tridentate ligand derived from aminoalcohols) were also found to be highly active. Although the [MoO<sub>2</sub>(SAP)] fragment (SAP = salicylideneaminophenolato) is stable during the process, other ONO tridentate Schiff base ligands suffered from hydrolysis under the reaction conditions. It was interesting to explore more deeply this model reaction using “old” but very stable and relatively simple compounds, the polyoxometalates (POMs), which do not have surrounding ligands that could potentially suffer from decomposition processes under the

aggressive reaction conditions.

POMs have been known for quite a long time<sup>16-19</sup> and have attracted interest as chromogenic devices and for applications to biological processes and to catalysis, including heterogeneous and homogeneous industrial processes.<sup>20-22</sup> They are very efficient catalysts for pulp bleaching or for the transformation of cellulose.<sup>23-25</sup> Oxidation reactions catalyzed by POMs usually work with several oxidants (H<sub>2</sub>O<sub>2</sub>, H<sub>2</sub>O<sub>2</sub>-urea, TBHP, O<sub>2</sub><sup>26, 27</sup>) and transform different substrates such as alcohols<sup>5, 28-32</sup> sulphur-containing compounds<sup>33-36</sup> and olefins.<sup>37-42</sup> Due to their robustness under a variety of experimental conditions, the most often used POMs in catalysis are the Keggin type,<sup>43-47</sup> particularly those containing tungsten since they generally show greater activity.<sup>48</sup> The stoichiometric oxidation of tungsten containing POMs leads to the generation of peroxido derivatives that are believed to be the active forms in catalysis. One of the most active systems is the so called Venturello catalyst, i.e. a peroxopolyoxotungstate of formula [PW<sub>4</sub>O<sub>24</sub>]<sup>3-</sup> obtained from [PW<sub>12</sub>O<sub>40</sub>]<sup>3-</sup> with excess H<sub>2</sub>O<sub>2</sub>. This anion has been used as a catalyst under phase transfer conditions in the presence of substituted imidazolium cations as transfer agents.<sup>49-52</sup> These catalytic reactions were mainly performed in the presence of an organic solvent, including Pickering emulsion systems.<sup>42</sup> One of the best systems is known as the Ishii-Venturello catalytic system, indicated by W<sup>VI</sup>/P<sup>V</sup>/H<sub>2</sub>O<sub>2</sub>/CHCl<sub>3</sub>/PTC (PTC = phase transfer catalyst).<sup>53, 54</sup>

Recently, solvent-free conditions were reported to yield good activity for the epoxidation of different olefins, especially cyclooctene, in the presence of a peroxopolyoxotungstate-based room temperature ionic liquid.<sup>12</sup> Other peroxotungstates exhibited interesting results in the presence of ethylacetate as solvent, which is less toxic than the chlorinated solvents that are more

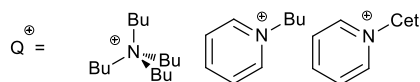
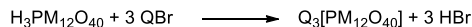
commonly used in this process.<sup>55, 56</sup> The molybdenum equivalent of formula  $[\text{PMo}_4\text{O}_{24}]^{3-}$  was shown to be an active catalyst under homogeneous conditions.<sup>57</sup> However, although it has been used in many catalytic applications such as oxygen transfer from sulfoxides,<sup>58</sup> methacrolein oxidation,<sup>59</sup> or the Meyer-Schuster rearrangement of propargyl alcohols,<sup>60</sup> the epoxidation of olefins in the presence of this catalyst has been poorly investigated.<sup>61</sup>

We present in this article the application of various salts of the  $[\text{PMo}_4\text{O}_{24}]^{3-}$  ion at low catalytic loading and under solvent-free conditions to the epoxidation of cyclooctene by both aqueous TBHP and  $\text{H}_2\text{O}_2$ . The determination of the kinetic profile and the evolution of the selectivity allow interesting considerations on the chemical environment of the catalytic transformation.

## Results and Discussion

### (a) Synthesis and characterization

The three phosphomolybdates salts of general formula  $\text{Q}_3[\text{PMo}_{12}\text{O}_{40}]$  [ $\text{Q} = \text{N}(n\text{-C}_4\text{H}_9)_4$  (tetra-*n*-butylammonium, TBA), *n*- $\text{C}_4\text{H}_9\text{NC}_5\text{H}_5$  (N-butylpyridinium, BP), *n*- $\text{C}_{16}\text{H}_{33}\text{NC}_5\text{H}_5$  (N-cetylpyridinium, CP)] and the phosphotungstate (BP)<sub>3</sub>[ $\text{PW}_{12}\text{O}_{40}$ ] are easily available by cation exchange from the commercially available fully protonated heteropolyacid  $\text{H}_3\text{PMo}_{12}\text{O}_{40}$  or  $\text{H}_3\text{PW}_{12}\text{O}_{40}$  and the corresponding organic bromide salt QBr, see Scheme 1. The TBA<sup>62</sup> and CP<sup>61</sup> salts have previously been described in the literature. The BP salt of the analogous phosphotungstate, (BP)<sub>3</sub>[ $\text{PW}_{12}\text{O}_{40}$ ] has also been prepared by the same strategy (see experimental part).



M = Mo (Q = TBA, CP, BP)  
W (Q = BP)

Scheme 1–X-Ray Structure of (BP)<sub>3</sub>PMo<sub>12</sub>O<sub>40</sub>. Hydrogen atoms were omitted for clarity.

The IR and NMR properties of the new BP salts are as expected (see Experimental section). In addition, a single crystal obtained for the (BP)<sub>3</sub>[PMo<sub>12</sub>O<sub>40</sub>] salt was analyzed by X-ray diffraction.

The molecular unit is composed of the well known Keggin  $[\text{PMo}_{12}\text{O}_{40}]^{3-}$  anion surrounded by three butylpyridinium cations (see Figure 1). All the bonding parameters in the trianion agree with those found in the structures of other salts containing the same POM anion and in the hydrated heteropolyacid.<sup>63-67</sup> There are no short contacts between cations and anion, the former lacking any active proton. The shortest anion-cation contact is 3.160 Å between C(35), a pyridinium ring carbon atom, and one of the terminal oxo atoms, O(241), for a calculated C(35)-H(35)-O(241) angle of 141°.

### (b) Catalytic studies

All synthesized salts have been tested as catalysts for the epoxidation of cyclooctene as model substrate, using either hydrogen peroxide (35 wt% in water) or TBHP (70 wt% in water)

as oxidant (Scheme 2), with emphasis on the less extensively investigated Mo species. The reaction was carried out at 80°C in the absence of any extra organic solvent, hence under aqueous biphasic conditions. As previously established, the TBHP oxidant partitions mainly in favour of the substrate phase under these conditions,<sup>15</sup> whereas  $\text{H}_2\text{O}_2$  remains in the aqueous phase.

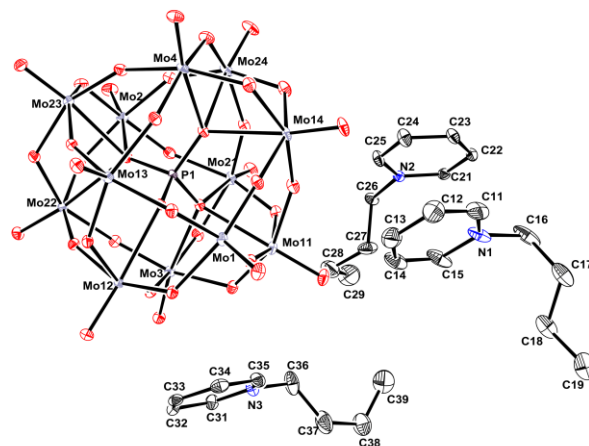
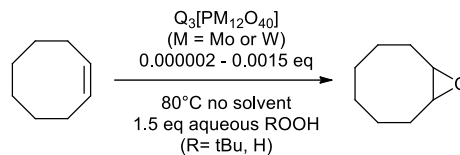


Figure 1–X-Ray Structure of (BP)<sub>3</sub>PMo<sub>12</sub>O<sub>40</sub>. Ellipsoids were drawn at the 30% probability level and hydrogen atoms were omitted for clarity.



Scheme 2–General scheme of the reaction.

The influence of cation and oxidant has been investigated by following the conversion and selectivity at a relatively low pre-catalyst loading (0.1 mol % vs. substrate) for 24 h, using an oxidant/substrate ratio of 1.5. The amount of catalyst is expressed in terms of POM content rather than metal content, since the number of catalytically active metal atoms in the anion is unclear. The POM salts appear totally insoluble in the reaction medium at room temperature, but partially dissolve at the reaction temperature in the substrate phase (see below for more details). The results of the kinetic monitoring are shown in Figure 2 (conversion) and Figure 3 (selectivity). All catalytic solutions gave a rapid phase separation when stirring was stopped, allowing the clean withdrawal of samples of the supernatant organic phase.

Most other reports of epoxidations catalyzed by POM compounds and notably those carried out under heterogeneous or homogeneous biphasic conditions report only the final conversion and selectivity data. As evidence in Figure 2, the profile under our conditions depends on oxidant and cation nature. An induction period was observed when using  $\text{H}_2\text{O}_2$ , longer for the TBA salt, intermediate for BP and not detectable for CP, whereas no induction period could be detected for any of the three salts when using TBHP. On the other hand, the activity for the oxidations with TBHP decreases in the order BP > CP > TBA.

Figure 3 shows that the selectivity also depends on the nature of the oxidant and cation. For the oxidations with TBHP, the epoxide selectivity is the range of 65-75% for all  $\text{Q}_3[\text{PMo}_{12}\text{O}_{40}]$

catalysts. The only other observed product is the *trans*-cyclooctane-1,2-diol and no isomeric *cis*-diol was detected. For the H<sub>2</sub>O<sub>2</sub> oxidations, on the other hand, the TBA and BP catalysts yield low selectivities (20-30%) from the very beginning of the reaction, the only other observed product being once again the *trans*-diol. The CP catalyst, on the other hand, yields an initially high selectivity, comparable to that of the TBHP oxidation, then decreasing at higher conversion toward values comparable to those obtained with the other catalysts.

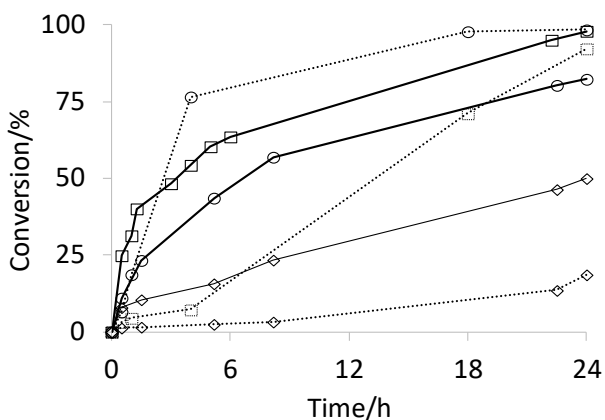


Figure 2 - Time dependence of the cyclooctene conversion in the presence of Q<sub>5</sub>[PMO<sub>12</sub>O<sub>40</sub>]. Q = BP (□) TBA (◇) CP (○). Oxidant = H<sub>2</sub>O<sub>2</sub> (dotted lines), TBHP (plain lines). Conditions: cyclooctene/oxidant/POM = 1000/1500/1. T= 80°C.

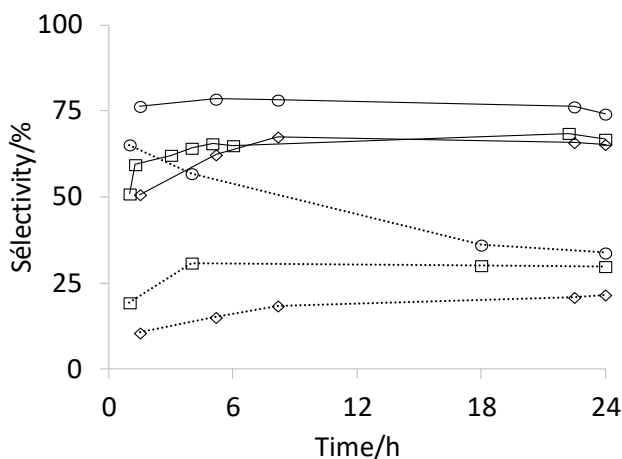


Figure 3- Cyclooctene oxide selectivity vs. time corresponding to the conversions shown in Figure 1 (same labels and lines as in Figure 1).

It should be remarked that the reactant and products were only analyzed in the organic layer. Cyclooctene and cyclooctene oxide are not strongly water soluble, therefore the determination of the epoxide selectivity (epoxide yield/cyclooctene conversion) from this measurement should be accurate. The diol product, on the other hand, partitions in both phases as also suggested by indirect observations (see later). Therefore, mass balance in the organic phase is not expected and indeed not observed (see fuller details below). We also cannot exclude the formation of other by-products that are entirely confined in the water phase or that do not travel through the GC column.

Where does the catalysis take place?

The rationalization of the trends shown in Figure 2 and Figure 3 requires an understanding of where the catalytic transformation takes place. The two most reasonable possibilities are a homogenous process catalyzed by the dissolved POM salt within the bulk of the reactant phase, and a heterogeneous process on the surface of the undissolved catalyst, since the solubility of both catalyst and substrate in water is negligible. The question is not a trivial one, because numerous reports exist of oxidation reactions (of olefin, alcohols, diols, ..) in organic solvents such as chloroform, benzene, tert-butanol, etc. by aqueous H<sub>2</sub>O<sub>2</sub> run under phase-transfer conditions, which is generally considered as a homogeneous phase process. This includes the use of (CP)<sub>3</sub>[PMO<sub>12</sub>O<sub>40</sub>] as oxidation catalyst.<sup>54, 61, 68-70</sup> However, a recent report on olefin epoxidation (including cyclooctene) by aqueous H<sub>2</sub>O<sub>2</sub> using toluene as solvent and (C<sub>12</sub>H<sub>25</sub>NMe<sub>3</sub>)<sub>3</sub>[PW<sub>12</sub>O<sub>40</sub>] as catalyst emphasized a heterogeneous process occurring at the water-organic interface of Pickering emulsions where the catalyst is located in the form of solid nanoparticles.<sup>42</sup> A significant solubility difference may of course exist between the dodecyltrimethylammonium salt of the phosphotungstate Keggin ion in toluene and the cetylpyridinium salt of the phosphomolybdate Keggin ion in neat cyclooctene.

In order to learn more about the catalyst solubility in the organic phase at the reaction temperature, recovery and recycling experiments were carried out, as well as catalytic runs at lower catalyst loading. From the experiments run under the conditions of Figure 2 (0.1% catalyst loading), the catalyst was recovered at the end of the reaction by filtration from the crude solutions. In the case of BP and TBA, > 85% of the catalyst was recovered from both the H<sub>2</sub>O<sub>2</sub> and the TBHP oxidation processes. A lower amount of solid (ca. 70%), on the other hand, was recovered from the experiments with the CP salt. This suggests a greater catalyst solubilisation of the CP salt in the organic phase, which appears consistent with the longer hydrophobic chain in the CP cation. The different catalyst solubility and the hypothesis of a homogeneous process would seem consistent with the higher activity of the CP catalyst for the epoxidation with H<sub>2</sub>O<sub>2</sub>, although it is slightly surpassed by the BP salt for the epoxidation with TBHP. The TBA salt, on the other hand, results in the lowest activity with both oxidants. Weak activity of TBA salts was already reported with other types of polyanions and directly linked to their lower solubility.<sup>47</sup> In order to rationalize the results on the basis of a heterogeneous process, it would be necessary to invoke a difference in active surface related to the granule size of the solid catalyst and/or in a counterion steric effect.

Catalytic runs for the epoxidation by TBHP with different catalyst loadings were carried out with the more active BP and CP salts by measuring the conversion and selectivity after 24 h at 80°C. The results are reported in Table 1 and illustrated in Figure 4. This investigation shows that significant conversions can be obtained even at extremely low catalyst loadings (down to 0.0002% or 2 ppm for the CP salt) for turnover frequencies up to 66000 h<sup>-1</sup> (18 s<sup>-1</sup>). A control experiment run under the same conditions without catalyst shows only a 6.5% conversion in 24 h with 29% epoxide selectivity. The positive effect of the catalyst, even at 2 ppm level, on activity and selectivity is therefore demonstrated. Figure 4 shows that the epoxide yield after 24 h is relatively independent on catalyst loading down to certain cutoff

value, which is much lower for the BP salt (0.002%) than for the CP salt (0.03%). The study confirms that the maximum conversion at 24 h is slightly greater for the BP salt (*cf.* Figure 1).

Table 1. Cyclooctene epoxidation by TBHP with different catalyst loadings.<sup>a</sup>

Catalyst	% cat.	% conv.	% sel.	TON	TOF (h <sup>-1</sup> )
(BP) <sub>3</sub> [PMo <sub>12</sub> O <sub>40</sub> ]	0.099	90.7	71.6	910	470
	0.010	85.2	72.1	8200	2500
	0.005	83.5	75.7	15000	5600
	0.002	79.4	75.3	40000	11000
	0.001	65.3	65.6	53000	16000
	0.0005	52.0	44.5	100000	35000
(CP) <sub>3</sub> [PMo <sub>12</sub> O <sub>40</sub> ]	0.149	77.7	78.0	520	140
	0.080	77.0	78.6	960	180
	0.030	82.0	79.4	2700	340
	0.004	66.7	67.5	15000	4100
	0.0005	51.2	47.1	100000	31000
	0.0002	44.4	53.1	220000	66000
-	-	6.5	29.0	-	-

<sup>a</sup> Conditions: TBHP/cyclooctene = 1.5, 24 h, 80°C.

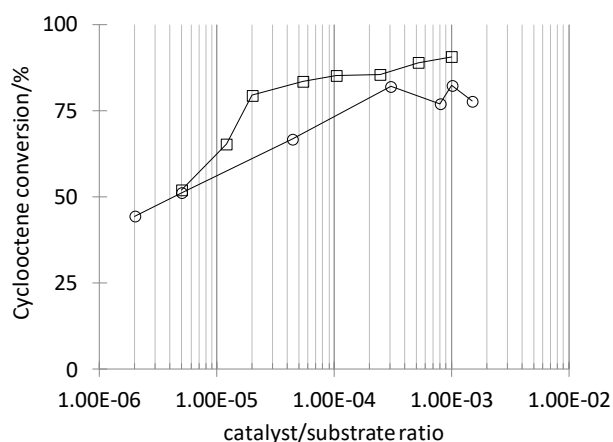


Figure 4- Cyclooctene epoxide yield after 24h vs. catalyst/cyclooctene ratio (data from Table 1). Q= BP (□)CP (○)

solubility, while the approximately constant conversion confirms the saturation effect discussed above.

Table 2. Recycle experiments for the cyclooctene epoxidation by TBHP.<sup>a</sup>

Complex	Run	% cat.	% conv.	% sel.
(TBA) <sub>3</sub> [PMo <sub>12</sub> O <sub>40</sub> ]	1	0.151	47.2	38.7
	2	0.098	50.7	38.5
	3	0.052	57.8	32.3
(BP) <sub>3</sub> [PMo <sub>12</sub> O <sub>40</sub> ]	1	0.099	90.7	71.6
	2	0.052	89.0	76.4
	3	0.025	85.5	74.8
(CP) <sub>3</sub> [PMo <sub>12</sub> O <sub>40</sub> ]	1	0.149	77.7	78.0
	2	0.101	82.3	74.1

<sup>a</sup> Conditions as in Table 2.

35

#### Rationalization of the selectivity

Turning now our attention on the question of the epoxide selectivity (Figure 3), the relatively low observed selectivity, even for the epoxidation by TBHP, contrasts with the high selectivity generally reported for reactions conducted in an organic solvent, for instance > 99% for both the phase transfer conditions with Venturello's system<sup>71</sup> and the Pickering emulsion system.<sup>42</sup> However, epoxides can be ring-opened in the presence of water, especially under acidic conditions. The pH of the aqueous phase during our catalytic runs was ca. 4 and did not change the course of the reaction. It is well known that the impact of the epoxide ring opening reaction is reduced when the epoxide is protected in a hydrophobic solvent where the water solubility is low and when the time of contact with the aqueous phase is limited.<sup>49</sup> No *cis* isomer that can potentially be obtained by concerted dihydroxylation could be detected; all diol formed under our conditions has the *trans* stereochemistry, therefore clearly resulting from the epoxide ring opening process.

The lower selectivity observed for the H<sub>2</sub>O<sub>2</sub> epoxidations can be rationalized by the greater amount of water (the aqueous H<sub>2</sub>O<sub>2</sub> solution has a lower concentration of oxidant - 30% - than the aqueous TBHP solution - 70%), leading to faster ring opening. In addition, the TBHP epoxidation produces *t*BuOH whereas the H<sub>2</sub>O<sub>2</sub> epoxidation produces additional water. The relatively constant selectivity with conversion observed in the TBHP case (Figure 3) probably results from compensation between additional epoxide formation and epoxide ring opening. Leaving the final reaction mixture for a longer time after complete cyclooctene conversion would certainly result in further ring opening with decrease of epoxide selectivity. For the oxidations with H<sub>2</sub>O<sub>2</sub>, the slower initial epoxidation with the TBA and BP salts also results in compensation of epoxide production and ring opening rates resulting in the observed relatively constant selectivity (Figure 3). On the other hand, the faster conversion obtained with the CP salt results in initially greater epoxide selectivity, similar to that of the epoxidations by TBHP, followed by a loss of selectivity when the ring opening process becomes more important. It is clear from these results that solvent-free conditions are not suitable when the desired product is the epoxide, but may provide advantages when the desired product is the *trans*-diol.

Further relevant information is provided by a more detailed analysis of the reaction conversion and selectivity at short reaction times for the reaction with H<sub>2</sub>O<sub>2</sub>. Figure 5 shows that

10 These results do not seem consistent with a fully heterogeneous process, for which the efficiency should be proportional to the active surface area and the yield would therefore be expected to reach 100% at higher loadings. Rather, they seem consistent with a saturation effect and a mostly homogeneous process. At loadings lower than the cutoff value, when all catalyst is presumably dissolved, the activity remains greater for the BP salt. This phenomenon may be caused by the cation steric effect since the dissolved catalyst presumably remains associated in the form of ion pairs at the higher concentrations. The two profiles, however, tend to converge at the lowest catalyst concentrations as may be expected for an equilibrated ion pair dissociation and catalytic action by the free POM ion.

15 A brief recycling study, run with catalytic loadings greater than the cut-off value of Figure 4, shows that the recovered catalyst is still active for all salts (Table 2). Incidentally, spectroscopic analyses (IR, <sup>1</sup>H and <sup>31</sup>P NMR) on the solids recovered at the end of the reactions confirmed the catalyst stability. The decreasing amount of solid catalyst recovered and used in subsequent recycles confirms the partial catalyst

formation of the epoxide product does not start immediately, whereas some cyclooctene is slowly converted even in the initial induction phase. However, *trans*-cyclooctane-1,2-diol is produced immediately, even though this is detected in very small amounts in the organic phase because most of it is retained in the aqueous phase. The continuous decrease with time of the total measured mass indicates the increasing production of water soluble product(s). More notable epoxide formation begins only at ca. 2 h from the start. Our interpretation of this phenomenon is that the initial slow cyclooctene consumption occurs by heterogeneous catalysis at the organic-water interface where, given the large presence of water, the epoxide is mostly opened to the diol. Subsequently, as more H<sub>2</sub>O<sub>2</sub> is able to migrate toward the bulk of the organic phase, the epoxide selectivity increases by virtue of the homogeneous process (see also next section).

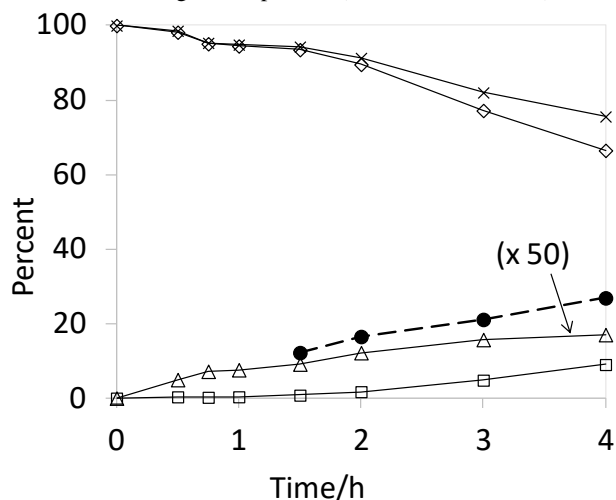


Figure 5- Time evolution of cyclooctene oxide yield (□), *trans*-cyclooctane-1,2-diol yield (Δ, x50), residual cyclooctene (◇), total (×), and cyclooctene oxide selectivity (● and dashed line) measured in the organic phase for the reaction of cyclooctene with H<sub>2</sub>O<sub>2</sub> (1.5 equiv) catalyzed by (BP)<sub>3</sub>[PMo<sub>12</sub>O<sub>40</sub>] (0.1%).

#### Rationalization of the induction period

The final question of interest related to the results of Figure 2 concerns the induction period and its dependence on the type of oxidant and cation. Clearly, the absence of an induction period for the TBHP epoxidations, where oxidant and catalyst are present in the reactant phase from the very beginning of the process, and its presence for the H<sub>2</sub>O<sub>2</sub> epoxidation, where the oxidant is initially present only in the aqueous phase, reinforces the idea that the catalyzed reaction mostly occurs in the bulk of the organic phase. Therefore, initial difficulty for the epoxidation by H<sub>2</sub>O<sub>2</sub> consists in bringing the oxidant into the organic phase. The presence of an induction period may be rationalized under the hypothesis that the products of the reaction (the epoxide and/or the diol) facilitate the H<sub>2</sub>O<sub>2</sub> transfer from the aqueous to the organic phase through a compatibilization effect.

In order to test this hypothesis, two additional catalytic experiments were carried out under the same conditions of the initial experiments for Figure 2 and Figure 3, in the presence of the (BP)<sub>3</sub>[PMo<sub>12</sub>O<sub>40</sub>] salt (0.1% catalyst, H<sub>2</sub>O<sub>2</sub>/substrate = 1.5), except for simulating a ca. 50% conversion at time zero by replacing part of the cyclooctene starting material with either cyclooctene oxide or *trans*-cyclooctane-1,2-diol (see Experi-

mental Section).

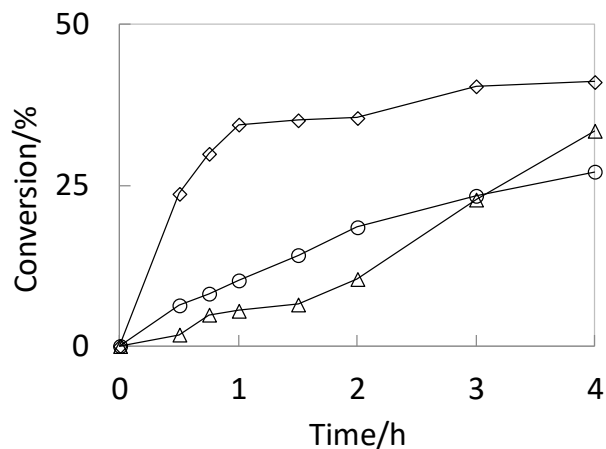


Figure 6- Cyclooctene conversion vs. time for the (BP)<sub>3</sub>[PMo<sub>12</sub>O<sub>40</sub>]-catalyzed epoxidation by aqueous H<sub>2</sub>O<sub>2</sub>. Conditions: (cyclooctene + additive)/H<sub>2</sub>O<sub>2</sub>/POM = 1000/1500/1. T= 80°C. Additive: none (Δ) (same as in Figure 2), cyclooctene oxide (○), *trans*-cyclooctane-1,2-diol (◇).

The results are shown in Figure 6 in comparison with those of the parent system (100 % cyclooctene). As can be seen from the kinetic profiles, the initial rate is slower in the presence of epoxide than in the presence of diol, but both transformations occur without a notable induction period. Hence, we can conclude that the induction period is indeed related to a compatibilization problem, rather than to the need for a catalyst activation phase. The reaction products, particularly the diol, have indeed a positive effect in increasing the concentration of the polar oxidant H<sub>2</sub>O<sub>2</sub> (and thus presumably also the water solvent) in the organic phase. Note that a rapid catalyst deactivation occurs in the presence of diol after ca. 1 h of reaction, before the conversion reaches the expected maximum of 50% (conversion is plotted with respect to the total maximum of moles, cyclooctene + additive, in order to directly compare the different runs). The conversion continues beyond this time, on the other hand, for the reaction carried out in the presence of the epoxide. Thus, the diol formation in the parent experiments of Figure 2 and Figure 3 has several effects, one being the acceleration of cyclooctene conversion through the oxidant transport into the cyclooctene phase, a second one being the acceleration of ring opening by also increasing the water concentration in the organic phase, and a third one being the catalyst deactivation.

Additional observations of interest are related to the selectivity and mass balance. The results of the monitoring of all concentrations in the organic phase for the two experiments are presented in Figure 7 for the experiment run in the presence of epoxide and in Figure 8 for the experiment run in the presence of diol. In the presence of epoxide, the diol formation starts once again immediately, but the epoxide production also occurs without induction time and to a much greater extent than that of the diol, with the initial epoxide selectivity being nearly 100%. The selectivity is calculated from the amount of epoxide produced in the reaction (and not the total amount) relative to the consumed cyclooctene. The mass balance is much better in this case relative to the experiment without additive (*cf.* with Figure

5), probably because the large amount of epoxide changes the solvent properties of the organic phase making it a better solvent for the diol relative to water.

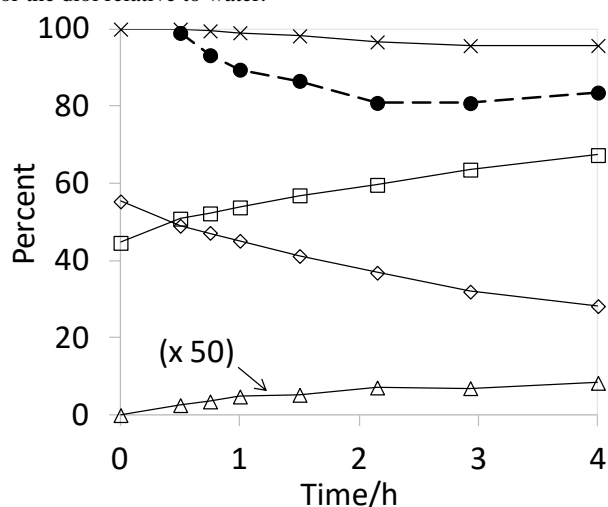


Figure 7- Time evolution of cyclooctene oxide yield (□), trans-cyclooctane-1,2-diol yield (Δ, x50), residual cyclooctene (◇), total cyclooctene oxide (×), and cyclooctene oxide selectivity (● and dashed line) measured in the organic phase for the reaction of cyclooctene in the presence of the cyclooctene oxide additive (cyclooctene/epoxide = 55:45). Other conditions as in Figure 6.

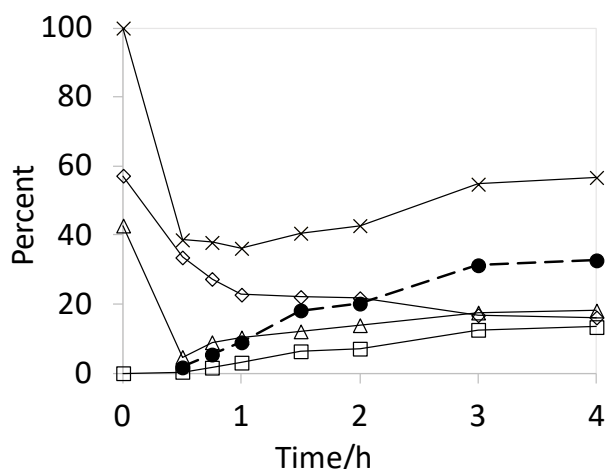


Figure 8- Time evolution of cyclooctene oxide yield (□), trans-cyclooctane-1,2-diol yield (Δ, x50), residual cyclooctene (◇), total cyclooctene oxide (×), and cyclooctene oxide selectivity (● and dashed line) measured in the organic phase for the reaction of cyclooctene in the presence of the trans-cyclooctane-1,2-diol additive (cyclooctene/diol = 57:43). Other conditions as in Figure 6.

In the presence of the diol, on the other hand, the mass balance is terrible, with a large amount of diol disappearing initially. This confirms that the diol affinity in a cyclooctene/water biphasic system is largely in favor of water. As the reaction progresses, on the other hand, the diol concentration in the organic phase increases again while the epoxide starts to form. The epoxide selectivity in this catalytic run is much lower, the reaction producing nearly only diol at the beginning and then increasing as the reaction progresses. In summary, the above experiments confirm the tendency of the epoxide to produce diol by ring opening in the presence of a large amount of diol and its little tendency when the organic phase is rich in epoxide and poor in

diol, consistent with the greater efficiency of the diol as a vector for bringing water into the organic phase.

The above described experiments rationalize the presence of an induction period for the  $H_2O_2$  epoxidation catalyzed by the TBA and BP salts, but does not explain why this phenomenon is absent when the same reaction is catalyzed by the CP salt (Figure 2). A possible explanation, which is supported by visual evidence, is that the longer hydrophobic chains of the CP cation are better able to stabilize micelles containing the substrate phase in the core and having the POM anions at the surface. Indeed, the reaction medium in the presence of the  $(CP)_3[PMo_{12}O_{40}]$  catalyst has the aspect of an emulsion, which phase separates much more slowly when stirring is stopped relative to the mixtures containing the TBA and BP catalysts. Therefore, the surface contact between the two phases is greatly increased and mass transport is accelerated relative to the stirred bulk phases in the presence of the other salts. The role of salts of POM anions as micelle stabilizing surfactants has also been described in the case of alcohol oxidation when performed in water/organic solvent biphasic systems.<sup>72</sup>

#### Influence of transition metal: Mo vs. W

In several processes involving Keggin polyanions, the tungsten salts have been described as more active than the molybdenum counterpart in the presence of  $H_2O_2$ , although the opposite trend has been reported for oxidations with TBHP.<sup>70, 73</sup> We wished to establish whether the same trend remains valid under solvent free conditions. Hence, analogous epoxidation processes to those described in Figure 2 were also run with both  $H_2O_2$  and TBHP using the BP salt of the  $[PW_{12}O_{40}]$  ion.

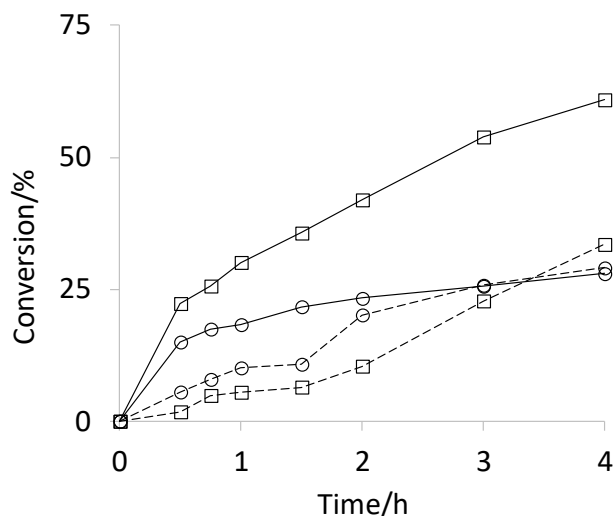


Figure 9- Cyclooctene conversion vs time for the cyclooctene epoxidation in presence of  $(BP)_3[PM_{12}O_{40}]$ . M = Mo (□), W (○); oxidant =  $H_2O_2$  (dotted lines) TBHP (plain lines). Conditions: cyclooctene/oxidant/POM = 1000/1500/1, T = 80°C.

As shown in Figure 9, the  $(BP)_3[PW_{12}O_{40}]$  salt indeed performs more poorly than the Mo analogue in combination with TBHP and better than the Mo analogue in combination with  $H_2O_2$ . The differences, however, are not dramatic. A similar induction effect appears to be present for the  $H_2O_2$  epoxidation catalyzed by the W species.

## Conclusions

We have described in this article the use of three salts of the  $[\text{PMo}_{12}\text{O}_{40}]^{3-}$  ion with tetrabutylammonium (TBA), butylpyridinium (BP), and cetylpyridinium (CP), as well as the BP salt of the analogous tungsten complex  $[\text{PW}_{12}\text{O}_{40}]^{3-}$ , in the epoxidation of cyclooctene under solvent-free conditions. The phosphomolybdate compounds, particularly those with the BP and CP cations, show very high catalytic activity, the highest measured TOF being in excess of  $60000\text{ h}^{-1}$  at 2 ppm catalyst loading for the CP salt and can be recycled when used in sufficiently large amount to exceed the solubility limit. The investigation gives compelling evidence in favour of a homogeneous process occurring in the bulk of the organic phase. However, the use of water as the carrier of the oxidizing reagent (and also formed as a co-product when using  $\text{H}_2\text{O}_2$ ) lead to significant epoxide ring opening to yield the *trans*-diol. Thus, solvent free conditions in combination with aqueous solution of the oxidant are not recommended when high epoxide selectivities are desired. The observed induction period for the  $\text{H}_2\text{O}_2$  oxidations has been demonstrated to be related to mass transport limitations for the  $\text{H}_2\text{O}_2$  reagent, these being attenuated by the presence of the epoxide product and especially by the diol product of further ring opening, which act as phase compatibilizers. The  $(\text{BP})_3[\text{PW}_{12}\text{O}_{40}]$  salt yield results quite comparable with those of the Mo analogue, being slightly less efficient for the epoxidation by TBHP and more efficient when using  $\text{H}_2\text{O}_2$ .

## Experimental part.

### Starting materials

All preparations were carried out in air. Compounds  $\text{H}_3[\text{PMo}_{12}\text{O}_{40}]\cdot 26\text{H}_2\text{O}$  (99.9%, Merck),  $\text{H}_3[\text{PW}_{12}\text{O}_{40}]\cdot 15\text{H}_2\text{O}$  (purum, Aldrich) were used as received, after having determined the water content by TGA. Tetrabutylammonium bromide (Aldrich, 99%), n-butylpyridinium bromide (Fluka, >99%), cetylpyridinium bromide (Aldrich, 98%), cyclooctene (Aldrich, 95%), cyclooctene oxide (Aldrich, 99%), *trans*-cyclooctane-1,2-diol (Alfa Aesar, 85%), TBHP (ACROS, 70% in water)  $\text{H}_2\text{O}_2$  (ACROS, 35% in water), diethylether (Sigma Aldrich, 99%) and  $\text{MnO}_2$  were used as received. Compound  $(\text{TBA})_3[\text{PMo}_{12}\text{O}_{40}]$  was synthesized by the literature procedure from  $\text{H}_3\text{PMo}_{12}\text{O}_{40}$  and  $\text{TBABr}$  in water.<sup>62</sup>

### Instrumentation

Infrared spectra were recorded in KBr matrices at room temperature with a Mattson Genesis II FTIR spectrometer or using the ATR mode with a Nicolet FTIR spectrometer.  $^1\text{H}$  and  $^{31}\text{P}$  NMR spectra were recorded on a Bruker Avance DPX-200 spectrometer. Catalytic reactions were followed by gas chromatography on an Agilent 6890A chromatograph equipped with FID detector, a capillary column (either an HP5-MS,  $30\text{ m} \times 0.25\text{ mm} \times 0.25\text{ }\mu\text{m}$ ; or an SE-30,  $30\text{ m} \times 0.32\text{ mm} \times 0.25\text{ }\mu\text{m}$ ) and automatic sampling. The GC parameters were quantified with authentic samples of the reactants and products. The conversion of *cis*-cyclooctene and the formation of cyclooctene oxide were calculated from calibration curves ( $r^2 = 0.999$ ) relatively to an internal standard.

### Synthesis of $(\text{BP})_3[\text{PMo}_{12}\text{O}_{40}]$

Using  $\text{To}$  2.00 g (0.87 mmol)  $\text{H}_3[\text{PMo}_{12}\text{O}_{40}]\cdot 26\text{H}_2\text{O}$  in 4 mL was added  $(\text{BP})\text{Br}$  (0.56 g, 2.62 mmol) in 2 mL water. A yellow precipitate formed very rapidly. The mixture was left stirring a few hours and then the precipitate was recovered by filtration, washed with water, diethyl ether and dried under vacuum at  $70^\circ\text{C}$  overnight. Yield: 1.89 g (97%). Yellow crystals were grown from a DMSO solution upon standing at room temperature over one week.  $^1\text{H}$  NMR ( $d_6$ -DMSO):  $\delta$  9.12 (d, 2H), 8.64 (t, 1H), 8.18 (t, 2H), 4.63 (t, 2H), 1.93 (q, 2H), 1.32 (m, 2H), 0.94 (t, 3H).  $^{31}\text{P}$  NMR ( $d_6$ -DMSO):  $\delta$  -2,88. IR ( $\text{cm}^{-1}$ ): 1064 (P=O) 962, 956 (Mo=O) 875, 791, 760 (Mo-O-Mo) 680 (pyridinium) Anal. Calcd for  $\text{C}_{27}\text{H}_{42}\text{Mo}_{12}\text{N}_3\text{O}_{40}\text{P}$  ( $M_r = 2230.87$ ): C, 14.5; H, 1.9; N, 1.9 Found: C, 14.6; H, 1.6; N, 1.7.

### Synthesis of $(\text{CP})_3[\text{PMo}_{12}\text{O}_{40}]$

This preparation was carried out by the same procedure described above for the BP salt, except for using ethanol as the solvent carrier of  $(\text{CP})\text{Br}$ .  $\text{H}_3[\text{PMo}_{12}\text{O}_{40}]\cdot 26\text{H}_2\text{O}$  (2.00 g, 0.87 mmol) in 10 mL water and  $(\text{CP})\text{Br}$  (1.05 g, 2.62 mmol) in 15 mL ethanol yielded 2.06 g (86%) of product as a yellow powder.  $^1\text{H}$  NMR ( $d_6$ -DMSO):  $\delta$  9.11 (d, 2H), 8.63 (t, 1H), 8.18 (t, 2H), 4.62 (t, 2H), 2.01-1.94 (m, 2H), 2.26 (s, 26H), 0.88 (t, 3H).  $^{31}\text{P}$  NMR ( $d_6$ -DMSO):  $\delta$  -2.86. IR ( $\text{cm}^{-1}$ ): 1060 (P=O) 968, 950 (Mo=O) 875, 794, 764 (Mo-O-Mo), 677 (pyridinium). Anal. Calcd for  $\text{C}_{63}\text{H}_{114}\text{Mo}_{12}\text{N}_3\text{O}_{40}\text{P}$  ( $M_r = 2735.82$ ): C, 27.6; H, 4.2; N, 1.5 Found: C, 27.6; H, 4.3; N, 1.5.

### Synthesis of $(\text{BP})_3[\text{PW}_{12}\text{O}_{40}]$

Using the same method B described above for the BP salt of  $[\text{PMo}_{12}\text{O}_{40}]^{3-}$ ,  $\text{H}_3[\text{PW}_{12}\text{O}_{40}]\cdot 15\text{H}_2\text{O}$  (0.77 g, 0.24 mmol) in 4 mL water and  $(\text{BP})\text{Br}$  (0.56 g, 2.62 mmol) in 2 mL water yielded 0.45 g (57%) of product as a white powder.  $^1\text{H}$  NMR ( $d_6$ -DMSO):  $\delta$  9.05 (d, 2H), 8.59 (t, 1H), 8.14 (t, 2H), 4.59 (t, 2H), 1.90 (q, 2H), 1.29 (m, 2H), 0.91 (t, 3H).  $^{31}\text{P}$  NMR ( $d_6$ -DMSO):  $\delta$  -15.6. IR ( $\text{cm}^{-1}$ ): 1075 (P=O) 971, (W=O) 888, 747 (W-O-W) 678 (pyridinium). Anal. Calcd for  $\text{C}_{27}\text{H}_{42}\text{W}_{12}\text{N}_3\text{O}_{40}\text{P}$  ( $M_r = 3285.31$ ): C, 9.9; H, 1.3; N, 1.3 Found: C, 10.1; H, 1.6; N, 1.6.

### Crystal Structure determination

A single crystal was mounted under inert perfluoropolyether at the tip of a glass fibre and cooled in the cryostream of an Oxford-Diffraction XCALIBUR CCD diffractometer. The data were collected using monochromatic  $\text{MoK}\alpha$  radiation ( $\lambda = 0.71073\text{ \AA}$ ). The structure was solved by direct methods (SIR97)<sup>74</sup> and refined by least-squares procedures on  $F^2$  using SHELXL-97.<sup>75</sup> All H atoms were introduced at idealized positions and treated as riding on their parent C atoms. The drawing of the molecules was realised with the help of ORTEP3.<sup>76, 77</sup> Crystal data and refinement parameters are shown in Table 3. Fractional atomic coordinates are given in Table S1 and bond distances and angles in Table S2 of the Supplementary Section. Crystallographic data (excluding structure factors) for the structure reported in this paper have been deposited with the Cambridge Crystallographic Data Centre as supplementary publication CCDC 938809. Copies of the data can be obtained free of charge on application to CCDC, 12 Union Road, Cambridge CB2 1EZ, UK [Fax: int. Code +44(1223)336-033; E-mail: deposit@ccdc.cam.ac.uk].

**Table 3.** Crystal data for (BP)<sub>3</sub>[PMo<sub>12</sub>O<sub>40</sub>]

Empirical formula	[Mo <sub>12</sub> O <sub>40</sub> P] (C <sub>9</sub> H <sub>14</sub> N) <sub>3</sub>
Formula weight	2230.89
Temperature, K	180(2)
Wavelength, Å	0.71073
Crystal system	Monoclinic
Space group	P 2 <sub>1</sub> /n
a, Å	11.9672(3)
b, Å	18.6128(4)
c, Å	24.1420(5)
α, °	90.0
β, °	96.754(2)
γ, °	90.0
Volume, Å <sup>3</sup>	5340.1(2)
Z	4
Density (calc), Mg/m <sup>3</sup>	2.775
Abs. coefficient, mm <sup>-1</sup>	2.854
F(000)	4256
Crystal size, mm <sup>3</sup>	0.447 x 0.311 x 0.254
Theta range, °	2.90 to 27.48
Reflections collected	54250
Indpt reflections (R <sub>int</sub> )	12008 (0.0297)
Completeness, %	97.9
Absorption correction	Multi-scan
Max. and min. transmission	1.0 and 0.668
Refinement method	F <sup>2</sup>
Data	12008 / 0 / 751
/restraints/parameters	
Goodness-of-fit on F <sup>2</sup>	1.153
R1, wR2 [I>2σ(I)]	0.0311, 0.0653
R1, wR2 (all data)	0.0362, 0.0676
Residual density, e.Å <sup>-3</sup>	1.854 / -1.231

### Catalytic Procedures

#### (a) Standard catalytic runs

In a typical experiment, cyclooctene (1 equiv) and Q<sub>3</sub>[PM<sub>12</sub>O<sub>40</sub>] (x equiv, see tables) were mixed together in a round bottom flask and stirred in air. Acetophenone was added as internal standard. The reaction temperature was regulated at 80°C and then 1.5 equiv of aqueous THBP or aqueous H<sub>2</sub>O<sub>2</sub> was added to the mixture under stirring, setting the zero reaction time. Samples of the organic phase were periodically withdrawn after stopping stirring and phase separation (liquid/liquid/solid), which was rapid for the TBA and BP salts, slower but still allowing withdrawal of the clear organic phase for the CP salt. For each aliquot, the reaction was quenched by addition of MnO<sub>2</sub>, followed by the addition of diethylether and removal of the manganese oxide and residual water by filtration through silica before GC analysis.

#### (b) Catalytic runs in the presence of additives

*With cyclooctene oxide.* The procedure was identical to that described in the previous section, except for use of 0.55 equiv cyclooctene and 0.45 equiv of cyclooctene oxide, with 0.01 equiv of (BP)<sub>3</sub>[PMo<sub>12</sub>O<sub>40</sub>]. The experiment was run with 1.5 equiv of H<sub>2</sub>O<sub>2</sub>.

*With trans-cyclooctane-1,2-diol.* The same procedure was again followed, this time starting from 0.57 equiv of cyclooctene and 0.43 equiv of trans-cyclooctane-1,2-diol.

#### (c) Recovery Procedure

At the end of a typical catalytic run as described above run with a

0.1% POM/substrate ratio, the solid was recovered by direct filtration of the reaction mixture at room temperature. The solid was then rinsed with water, ethanol and diethyl ether, and then dried and weighted (see Results). For each salt, the spectroscopic analyses of the recovered solids revealed no change relative to the introduced material.

### Acknowledgements

We acknowledge the Centre National de la Recherche Scientifique (CNRS) and the Institut Universitaire de France (IUF) for financial support, the Université Paul Sabatier and its Institut Universitaire Technologique for the facilities, and the European Union for the ERASMUS mobility fellowships of D.M.F. We thank Audric Michelot and Weili Wang for technical assistance.

### Notes and references

- <sup>a</sup> CNRS; LCC (Laboratoire de Chimie de Coordination); Université de Toulouse; UPS, INPT, 205, route de Narbonne, F-31077 Toulouse, France Fax: +33-561553003 Email : rinaldo.poli@lcc-toulouse.fr
- <sup>b</sup> Université de Toulouse; Institut Universitaire de Technologie Paul Sabatier - Département de Chimie, Av. Georges Pompidou, BP 20258, F-81104 Castres Cedex, France. E-mail: dominique.agustin@iut-tilse3.fr.
- <sup>c</sup> Institut Universitaire de France 103, bd Saint-Michel, 75005 Paris, France
- P. Anastas and J. Warner, *Green Chemistry: Theory and Practice*, Oxford University Press, New York, 1998.
  - P. Tundo, P. Anastas, D. S. Black, J. Breen, T. Collins, S. Memoli, J. Miyamoto, M. Polyakoff and W. Tumas, *Pure Appl. Chem.*, 2000, **72**, 1207-1228.
  - R. A. Sheldon, I. Arends and U. Hanefeld, *Green Chemistry and Catalysis*, Wiley-VCH, Weinheim, 2007.
  - Regulation (EC) n° 1907/2006 of the European Parliament and Of the Council, Official Journal of the European Union 30.12.2006, L396.
  - K. Sato, M. Aoki, J. Takagi and R. Noyori, *J. Am. Chem. Soc.*, 1997, **119**, 12386-12387.
  - P. U. Maheswari, P. de Hoog, R. Hage, P. Gamez and J. Reedijk, *Adv. Synth. Catal.*, 2005, **347**, 1759-1764.
  - X. Y. Shi and J. F. Wei, *J. Mol. Catal. A*, 2005, **229**, 13-17.
  - G. Noguera, J. Mostany, G. Agrifoglio and R. Dorta, *Adv. Synth. Catal.*, 2005, **347**, 231-234.
  - Y. Luan, G. Wang, R. L. Luck, M. Yang and X. Han, *Chem. Lett.*, 2007, **36**, 1236-1237.
  - T. M. A. Shaikh and A. Sudalai, *Eur. J. Org. Chem.*, 2008, 4877-4880.
  - E. Poli, J. M. Clacens, J. Barrault and Y. Pouilloux, *Catal. Today*, 2009, **140**, 19-22.
  - H. Li, Z. S. Hou, Y. X. Qiao, B. Feng, Y. Hu, X. R. Wang and X. G. Zhao, *Catal. Commun.*, 2010, **11**, 470-475.
  - C. Cordelle, D. Agustin, J.-C. Daran and R. Poli, *Inorg. Chim. Acta*, 2010, **364**, 144-149.
  - J. Pisk, D. Agustin, V. Vrdoljak and R. Poli, *Adv. Synth. Catal.*, 2011, **353**, 2910-2914.
  - J. Morlot, N. Uytbroeck, D. Agustin and R. Poli, *ChemCatChem*, 2013, **5**, 601-611.
  - Special Issue on Polyoxometalates (Ed.: C. L. Hill), *Chem. Rev.* 1998, **98**.

17. P. Gouzerh and A. Proust, *Chem. Rev.*, 1998, **98**, 77-111.
18. A. Proust, R. Thouvenot and P. Gouzerh, *Chem. Commun.*, 2008, 1837-1852.
19. D. Agustin, J. Dallery, C. Coelho, A. Proust and R. Thouvenot, *J. Organomet. Chem.*, 2007, **692**, 746-754.
20. K. I. Matveev, *Kinet. Katal.*, 1977, **18**, 862-877.
21. N. Mizuno, K. Yamaguchi and K. Kamata, *Coord. Chem. Rev.*, 2005, **249**, 1944-1956.
22. Y. F. Song and R. Tsunashima, *Chem. Soc. Rev.*, 2012, **41**, 7384-7402.
23. I. A. Weinstock, R. H. Atalla, R. S. Reiner, M. A. Moen, K. E. Hammel, C. J. Houtman, C. L. Hill and M. K. Harrup, *J. Mol. Catal. A*, 1997, **116**, 59-84.
24. A. R. Gaspar, J. A. F. Gamelas, D. V. Evtuguin and C. P. Neto, *Green Chem.*, 2007, **9**, 717-730.
25. J. Z. Zhang, X. Liu, M. Sun, X. H. Ma and Y. Han, *ACS Catal.*, 2012, **2**, 1698-1702.
26. Y. Nishiyama, Y. Nakagawa and N. Mizuno, *Angew. Chem. Engl.*, 2001, **40**, 3639-3641.
27. S. Farhadi and Z. Momeni, *J. Mol. Catal. A*, 2007, **277**, 47-52.
28. K. Sato, J. Takagi, M. Aoki and R. Noyori, *Tetrahedron Lett.*, 1998, **39**, 7549-7552.
29. P. Desrosiers, A. Guram, A. Hagemeyer, B. Jandeleit, D. M. Poojary, H. Turner and H. Weinberg, *Catal. Today*, 2001, **67**, 397-402.
30. R. Ben-Daniel, P. Alsters and R. Neumann, *J. Org. Chem.*, 2001, **66**, 8650-8653.
31. D. Sloboda-Rozner, P. L. Alsters and R. Neumann, *J. Am. Chem. Soc.*, 2003, **125**, 5280-5281.
32. A. M. Khenkin, L. J. W. Shimon and R. Neumann, *Inorg. Chem.*, 2003, **42**, 3331-3339.
33. Y. Sasaki, K. Ushimaru, K. Iteya, H. Nakayama, S. Yamaguchi and J. Ichihara, *Tetrahedron Lett.*, 2004, **45**, 9513-9515.
34. Z. E. Abdalla, B. S. Li and A. Tufail, *Colloids Surf., A*, 2009, **341**, 86-92.
35. H. Y. Lu, Y. N. Zhang, Z. X. Jiang and C. Li, *Green Chem.*, 2010, **12**, 1954-1958.
36. X. L. Xue, W. Zhao, B. C. Ma and Y. Ding, *Catal. Commun.*, 2012, **29**, 73-76.
37. D. C. Duncan, R. C. Chambers, E. Hecht and C. L. Hill, *J. Am. Chem. Soc.*, 1995, **117**, 681-691.
38. K. Kamata, K. Yonehara, Y. Sumida, K. Yamaguchi, S. Hikichi and N. Mizuno, *Science*, 2003, **300**, 964-966.
39. K. Kamata, M. Kotani, K. Yamaguchi, S. Hikichi and N. Mizuno, *Chem. Eur. J.*, 2007, **13**, 639-648.
40. L. Gharnati, O. Walter, U. Arnold and M. Doring, *Eur. J. Inorg. Chem.*, 2011, 2756-2762.
41. P. Jimenez-Lozano, I. D. Ivanchikova, O. A. Kholdeeva, J. M. Poblet and J. J. Carbo, *Chem. Commun.*, 2012, **48**, 9266-9268.
42. L. Leclercq, A. Mouret, A. Proust, V. Schmitt, P. Bauduin, J. M. Aubry and V. Nardello-Rataj, *Chem. Eur. J.*, 2012, **18**, 14352-14358.
43. J. F. Liu, P. G. Yi and Y. S. Qi, *J. Mol. Catal. A*, 2001, **170**, 109-115.
44. M. N. Timofeeva, Z. P. Pai, A. G. Tolstikov, G. N. Kustova, N. V. Selivanova, P. V. Berdnikova, K. P. Brylyakov, A. B. Shangina and V. A. Utkin, *Russ. Chem. B.*, 2003, **52**, 480-486.
45. D. Sloboda-Rozner and R. Neumann, *Green Chem.*, 2006, **8**, 679-681.
46. Y. Leng, J. Wang, D. R. Zhu, M. J. Zhang, P. P. Zhao, Z. Y. Long and J. Huang, *Green Chem.*, 2011, **13**, 1636-1639.
47. L. Hua, Y. X. Qiao, Y. Y. Yu, W. W. Zhu, T. Cao, Y. Shi, H. Li, B. Feng and Z. S. Hou, *New J. Chem.*, 2011, **35**, 1836-1841.
48. J. Hu and R. C. Burns, *J. Mol. Catal. A*, 2002, **184**, 451-464.
49. C. Venturello, E. Alneri and M. Ricci, *J. Org. Chem.*, 1983, **48**, 3831-3833.
50. C. Venturello and R. Dalosio, *J. Org. Chem.*, 1988, **53**, 1553-1557.
51. I. V. Kozhevnikov, G. P. Mulder, M. C. Steverink-de Zoete and M. G. Oostwal, *J. Mol. Catal. A*, 1998, **134**, 223-228.
52. Y. Ding, B. C. Ma, Q. Gao, G. X. Li, L. Yan and J. S. Suo, *J. Mol. Catal. A*, 2005, **230**, 121-128.
53. C. Venturello, R. Dalosio, J. C. J. Bart and M. Ricci, *J. Mol. Catal.*, 1985, **32**, 107-110.
54. Y. Ishii, K. Yamawaki, T. Ura, H. Yamada, T. Yoshida and M. Ogawa, *J. Org. Chem.*, 1988, **53**, 3587-3593.
55. Y. X. Qiao, Z. S. Hou, H. Li, Y. Hu, B. Feng, X. R. Wang, L. Hua and Q. F. Huang, *Green Chem.*, 2009, **11**, 1955-1960.
56. Y. Ding, W. Zhao, H. Hua and B. C. Ma, *Green Chem.*, 2008, **10**, 910-913.
57. L. Salles, C. Aubry, F. Robert, G. Chottard, R. Thouvenot, H. Ledon and J. M. Bregeault, *New J. Chem.*, 1993, **17**, 367-375.
58. A. M. Khenkin and R. Neumann, *J. Am. Chem. Soc.*, 2002, **124**, 4198-4199.
59. H. Kim, J. C. Jung, S. H. Yeom, K. Y. Lee and I. K. Song, *J. Mol. Catal. A*, 2006, **248**, 21-25.
60. M. Egi, M. Umemura, T. Kawai and S. Akai, *Angew. Chem. Engl.*, 2011, **50**, 12197-12200.
61. Y. Matoba, H. Inoue, J. Akagi, T. Okabayashi, Y. Ishii and M. Ogawa, *Synth. Commun.*, 1984, **14**, 865-873.
62. K. Nomiya, K. Yagishita, Y. Nemoto and T. A. Kamataki, *J. Mol. Catal. A*, 1997, **126**, 43-53.
63. C. J. Clark and D. Hall, *Acta Crystallogr., Sect. B: Struct. Sci.*, 1976, **32**, 1545-1547.
64. M. R. Spirelet and W. R. Busing, *Acta Crystallogr., Sect. B: Struct. Sci.*, 1978, **34**, 907-910.
65. M. M. Williamson, D. A. Bouchard and C. L. Hill, *Inorg. Chem.*, 1987, **26**, 1436-1441.
66. E. Coronado, J. R. Galan-Mascaros, C. Gimenez-Saiz, C. J. Gomez-Garcia, L. R. Falvello and P. Delhaes, *Inorg. Chem.*, 1998, **37**, 2183-2188.
67. L. H. Bi, E. B. Wang, L. Xu and R. D. Huang, *Inorg. Chim. Acta*, 2000, **305**, 163-171.
68. Y. Ishii, K. Yamawaki, T. Yoshida, T. Ura and M. Ogawa, *J. Org. Chem.*, 1987, **52**, 1868-1870.
69. K. Yamawaki, T. Yoshida, H. Nishihara, Y. Ishii and M. Ogawa, *Synth. Commun.*, 1986, **16**, 537-541.
70. Y. Ishii, T. Yoshida, K. Yamawaki and M. Ogawa, *J. Org. Chem.*, 1988, **53**, 5549-5552.
71. N. M. Gresley, W. P. Griffith, A. C. Laemmel, H. I. S. Nogueira and B. C. Parkin, *J. Mol. Catal. A*, 1997, **117**, 185-198.
72. R. Noyori, M. Aoki and K. Sato, *Chem. Commun.*, 2003, 1977-1986.
73. P. Sözen-Aktaş, E. Manoury, F. Demirhan and R. Poli, *Eur. J. Inorg. Chem.*, 2013, 2728-2735.

- 
74. A. Altomare, M. Burla, M. Camalli, G. Cascarano, C. Giacovazzo, A. Guagliardi, A. Moliterni, G. Polidori and R. Spagna, *J. Appl. Cryst.*, 1999, **32**, 115-119.
75. G. M. Sheldrick, *SHELXL97. Program for Crystal Structure refinement*, University of Göttingen, Göttingen, Germany, 1997.
76. M. N. Burnett and C. K. Johnson, *ORTEPIII, Report ORNL-6895*, Oak Ridge National Laboratory, Oak Ridge, Tennessee, U.S., 1996.
77. L. J. Farrugia, *J. Appl. Cryst.*, 1997, **30**, 565.